

Structure, Growth Process, and Growth Mechanism of Perovskite in High-Titanium-Bearing Blast Furnace Slag



LU LIU, MEILONG HU, YUZHOU XU, CHENGUANG BAI, and YUNHUA GAN

The isothermal crystallization of perovskite in $\text{TiO}_2\text{-CaO-SiO}_2\text{-Al}_2\text{O}_3\text{-MgO}$ high-titanium-bearing blast furnace slag was observed *in situ* at 1698 K (1425 °C) using a confocal scanning laser microscope. The dendrite structure of perovskite (CaTiO_3) thus obtained showed vividly the primary dendrite trunks and secondary dendrite arms. Furthermore, the dendritic growth of perovskite in liquid slag was clearly observed on line. The results showed that the dendrite arrays in which the primary dendrite trunks observed on slag surface were parallel with each other grew toward the same direction. The secondary dendrite arms grew in the perpendicular direction with the primary trunks and stopped growing when they encounter. The perovskite dendrites showed a linear growth at two stages. The dendrites grew faster at early stage at about 5 to 7 $\mu\text{m/s}$ and grew with a lower growth rate at about 1 to 2 $\mu\text{m/s}$ in later stage. Finally, the growth mechanism of perovskite in melt was analyzed with the solidification theory. Based on the theoretical calculation of equilibrium phases in slag, the initial slag could be considered as a binary component system. One component was perovskite and the other component was the sum of all the other species that did not attend the crystallization of perovskite (included SiO_2 , Al_2O_3 , and MgO , as well as CaO and TiO_2 that were not involved in the solid formation). The formation of perovskite required the diffusion of CaO and TiO_2 to the solid/liquid interface and the rejection of the other species from the interface. The solid/liquid equilibrium schematic diagram was made based on the calculation.

DOI: 10.1007/s11663-015-0350-x

© The Minerals, Metals & Materials Society and ASM International 2015

I. INTRODUCTION

THE Panzihua–Xichang area has abundant vanadium-titanium magnetite ores, which are the source of more than 90 pct titanium resource in China. Currently, after mineral separation and a blast furnace smelting process, more than 50 pct titanium in raw ores finally gathers in the blast furnace (BF) slag, making the titanium content in terms of TiO_2 in slag up to 23 pct (Figure 1).^[1] The high titanium content has a big influence on the use of the slag, especially the high melting point phase, the rich-titanium phase—perovskite (CaTiO_3) affects the slag property and titanium extraction.^[2,3] On the one hand, CaO mostly exists as perovskite with TiO_2 in high-titanium-bearing BF slag, which in turn makes the slag unsuitable to be used as cement like the normal BF slag. On the other hand, the extraction of valuable secondary titanium resource from the slag always faces challenges. Gathering titanium into

perovskite was once considered to be a promising technology.^[2] However, the perovskite yield is rather low because of the adverse effects of the fine and uneven perovskite grains on the mineral separation.^[4] Therefore, it is necessary to study the crystallization of perovskite in high-titanium-bearing blast furnace slag.

A confocal scanning laser microscope (CSLM) has been used successfully to study the high-temperature behavior of slag system. Jung and Sohn^[5] observed the crystallization behavior of a calcium-aluminate system with various MgO contents, $\text{CaO}/\text{Al}_2\text{O}_3$ ratios, and cooling rates using a CSLM. The results indicated a change in primary phase and crystal morphology from dendrites to faceted crystals to columnar crystals in the composition range. Jung and Sohn^[6] also investigated the effect of FeO concentration on the crystallization of high-temperature $\text{CaO-Al}_2\text{O}_3\text{-MgO-FeO}$ melts with a CSLM. Continuous-cooling-transformation (CCT) and time-temperature-transformation (TTT) diagrams were plotted for melts, and the morphology of the primary crystals formed was determined. Orrling *et al.*^[7] studied the role of alumina particle in $\text{SiO}_2\text{-CaO-Al}_2\text{O}_3\text{-MgO}$ slag by CSLM. Semykina *et al.*^[8] observed the crystal growth of liquid FeO-CaO-SiO_2 slag during oxidation by using the CSLM. Sridhar and Cramb^[9] described the kinetics of Al_2O_3 dissolution in the $\text{CaO-MgO-SiO}_2\text{-Al}_2\text{O}_3$ slag with a CSLM.

The crystallization of perovskite in high-titanium-bearing blast furnace slag during continuous cooling has

LU LIU and YUZHOU XU, Graduate Students, MEILONG HU, Associate Professor, CHENGUANG BAI, Professor, are with the College of Materials Science and Engineering, Chongqing University, Chongqing, 400044 P.R. China. YUNHUA GAN, Associate Professor, is with the School of Electric Power, South China University of Technology, Guangzhou 510640, P.R. China. Contact e-mails: hml@cqu.edu.cn; ganyh@scut.edu.cn

Manuscript submitted September 3, 2014.

Article published online May 27, 2015.

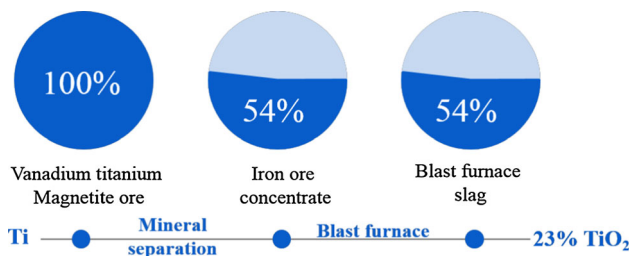


Fig. 1—The flow direction of titanium in blast furnace process.

been studied *in situ* by using confocal scanning laser microscopy in other previous work,^[4,10] which showed that the growth of perovskite proceeds *via* the successive production of quasi-particles along straight lines on the slag surface, and finally presented dendrites. However, the nucleation and actual growth process of dendrites were not observed because the quasi-particles were presumptively the successive appearances of the secondary dendrite tips that grew from the primary dendrites that had nucleated and grown from the crucible bottom with lower temperature under non-isothermal condition. In the current study, the isothermal crystallization experiment of perovskite in synthesized high-titanium-bearing BF slag was carried out to observe the growth process of perovskite dendrites, understand the distribution of temperature field, and concentration field of the growing dendrite tips. In addition, the growth mechanism of perovskite was investigated by using the binary alloy crystallization model based on the classic solidification theory.

II. EXPERIMENTAL PROCEDURE

A. Thermodynamic Calculation

The equilibrium phases of the synthesized titanium-bearing slag at different temperatures were calculated by using FactSage 6.3 (Thermfact/CRCT, Montréal, Canada) (Figure 2).^[11] According to the equilibrium phase diagram, the solidification point of the melt slag is 1709 K (1436 °C). At this temperature, perovskite is predicted to be the primary phase crystallizing from liquid slag during cooling. Table I shows the starting crystallization temperature and mass percent of the crystalline phase.

B. Materials and Sample Preparation

To simplify the crystallization process and eliminate the impact of minor phases in industry slag such as TiC, the synthesized slag, which was prepared by premelting 100 g of chemical reagent-grade CaO (98 pct), MgO (98 pct), SiO₂ (99 pct), TiO₂ (99 pct) and Al₂O₃ (98 pct) powder mixture with the aim composition refer to the industrial slag composition as shown in Table II, was used in the experiment. The chemical reagent powder was mixed after drying at 373 K (100 °C) for 6 hours. Then, 100 g mixed powder was put into a molybdenum crucible (50 mm inner diameter and 80 mm height) and melted

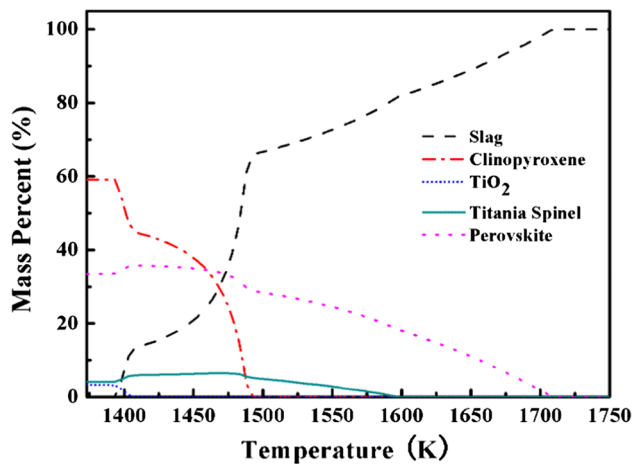


Fig. 2—Theoretical isothermal phase composition of the synthesized slag calculated by using FactSage.

under an argon atmosphere at 1773 K (1500 °C) for 1 hour in a MoSi₂ furnace so that the slag was homogenized. After melting, the slag was cooled against a copper plate. Subsequently, the slag was broken, incised, and polished into small slag samples into a wafer shape of 7 mm in diameter and 3 mm in height for running the experiment. Before the CSLM experiment, the slag sample was cleaned in an ultrasonic cleaning apparatus for 10 minutes. The slag was also analyzed by X-ray fluoroscopy (XRF), and the result in Table II shows that there is small deviation with the designed composition.

C. Apparatus and Procedure

The crystallization of perovskite in synthesized titanium-bearing BF slag was observed *in situ* by using a CSLM equipped with an infrared furnace (model: VL2000DX; Lasertec Corporation, Yokohama, Japan) which enables real-time *in situ* observation at a high temperature [up to 1973 K (1700 °C)] of transient phenomena. The melting and solidification of the slag sample took place in a platinum crucible (inner diameter of 8 mm and height of 5 mm) under an argon atmosphere in the CSLM (Ar > 99.999 pct). The platinum crucible was put on a platinum holder equipped with an R-type thermocouple in the infrared furnace. The halogen lamp irradiates light toward the golden cladding layer inside the reaction furnace chamber and then the layer reflects the energy toward the focal plane to heat the slag sample rapidly. Prior to heating, the infrared furnace was evacuated and backfilled with argon alternatively three times to remove the air from the furnace. The moisture and oxygen contents in the argon were removed by using the purifier provided with the CSLM. After the sample reached thermal equilibrium, the melt was cooled at a controlled rate, and video images of the slag surface were collected (25 frames per second, 1920 × 1080). The temperature and time were recorded on the images, and this information was later used to analyze the results. The schematic diagram of CSLM is shown in Figure 3. The temperature accuracy was confirmed by melting experiments of pure copper

Table I. The Theoretical Crystallization Temperature, Composition, and Final Mass Percent of the Crystalline Phase Calculated by Using FactSage in Fig. 2

Phase	Crystallization Temperature [K (°C)]	Composition	Final Mass Pct
Perovskite	1709 (1436)	Ca ₂ Ti ₂ O ₆	33.54
Titanium spinel	1598 (1325)	MgAl ₂ O ₄	4.11
Clinopyroxene	1489 (1216)	CaMgSi ₂ O ₆	59.09
TiO ₂	1395 (1122)	TiO ₂	3.26

Table II. Chemical Composition of the Industrial Slag and the Experimental Synthesized Slag (Weight Percent)

Slag Type	TiO ₂	CaO	SiO ₂	Al ₂ O ₃	MgO	MoO ₃	Total
Industrial slag	22.34	26.96	24.21	14.35	8.32	0	96.18
Synthesized slag	23	28.8	26.2	14	8	0	100
Composition, as analyzed using XRF	22.42	28.79	25.40	14.28	7.64	1.47	100

*In the XRF result, the trace impurities (Fe, K, P, Cr, C, and N) were ignored and the major species were normalized to give a total of 100 pct. It was assumed that MoO₃ had little effect on the experiments.

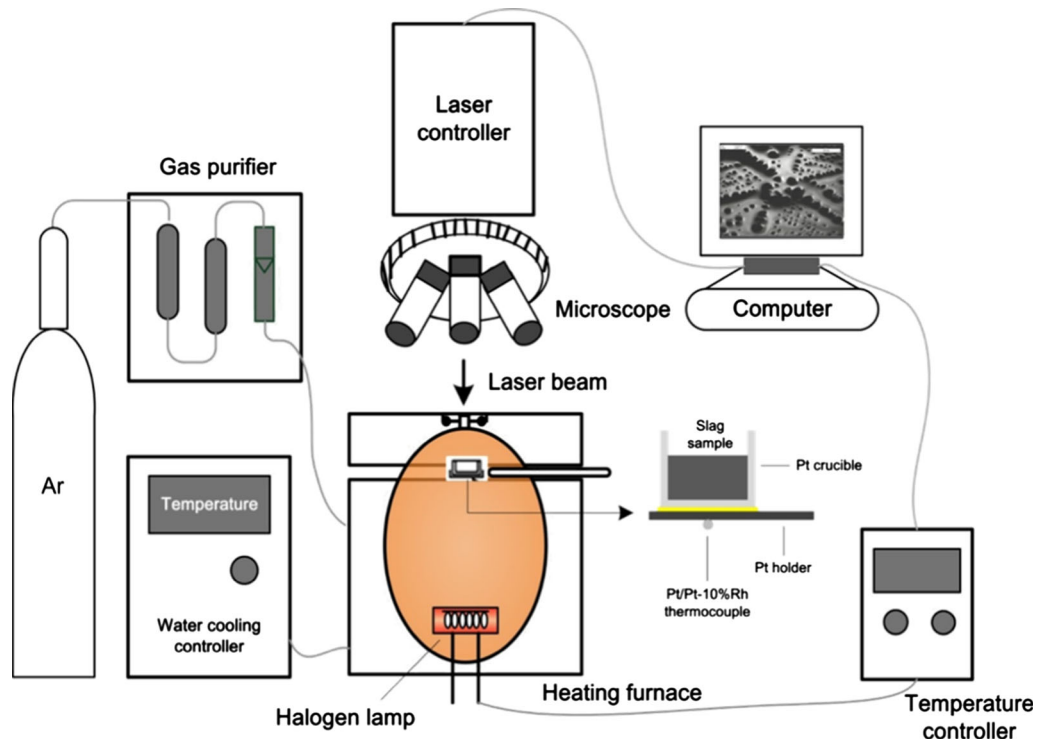


Fig. 3—The schematic diagram of confocal scanning laser microscopy.

[melting point: 1356 K (1083 °C)] and pure nickel [melting point: 1726 K (1453 °C)]. To get the growth process of perovskite, a small undercooling based on the theoretical calculation was set to get close to the isothermal crystallization condition. The temperature schedule is shown in Figure 4. The slag sample was heated to 1773 K (1500 °C) at a fixed heating rate of 300 K/min and was held for 2 minutes. Then, the slag was cooled to 1698 K (1425 °C) at a rate of 600 K/min and maintained for enough time to observe the crystallization of perovskite in the slag. The undercooling is:

$$\Delta T = 1709 \text{ K (1436 °C)} - 1698 \text{ K (1425 °C)} = 11 \text{ K (11 °C)}.$$

Generally, in an undercooled melt, equiaxed dendritic crystals form that are expected to be observed and the latent heat of fusion is dissipated through the cooler liquid ahead of the interface.^[12]

Furthermore, the cooled sample was examined using scanning electron microscope (SEM; TESCAN VEGA II) in back scattered electron (BSE) mode. The chemical

composition and phase of the samples were analyzed by using an energy-dispersive X-ray spectrometer (INCA Energy 350; Oxford Instruments, Oxfordshire, U.K.) equipped with the SEM and X-ray diffraction (XRD; D/max 2500PC; Rigaku Corporation, Tokyo, Japan), respectively.

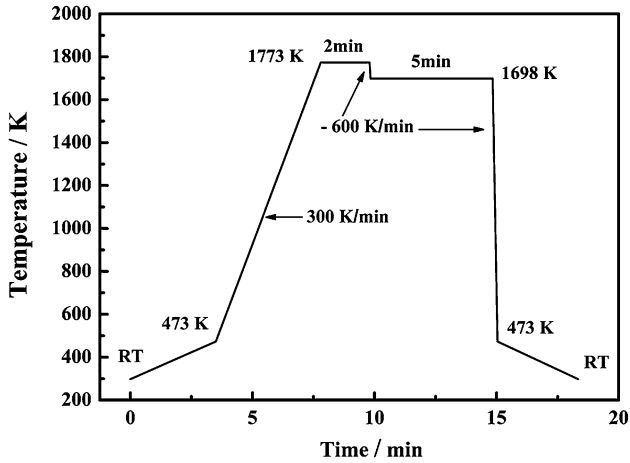


Fig. 4—The temperature schedule of CSLM experiment.

III. RESULTS AND DISCUSSION

A. Structure and Growth Process of Perovskite Dendrites

The growth process of perovskite can be clearly observed *via* CSLM and recorded in a video (25 frames per second, 1920×1080). Figure 5 shows the growth process of perovskite dendrites at 1698 K (1425 °C)

The dendrite-phase perovskite is confirmed by the XRD analysis (Figure 6). It shows that in the growing dendrite arrays, the primary dendrite trunks are parallel with each other and grow toward the same direction like the number 1 and 2 dendrites in Figure 5. At the same time, the secondary branches grow in the perpendicular direction with the primary trunk. Their growths are ceased when they encounter with each other.

The SEM images (Figure 7) present the dendrite arrays and equiaxed dendrites with a clearer outline. The primary dendrite trunks are parallel with each other just like the growing dendrites in Figure 5.

In the previous study of the continuous-cooling crystallization of perovskite at different cooling rates, the three-dimensional structures of perovskite dendrites were obtained.^[10] In case of the crystallization process corresponding to the cooling rate of 10 K/min, because the solidification of perovskite consumed the liquid, the liquid drained and some voids remained in solidified slag

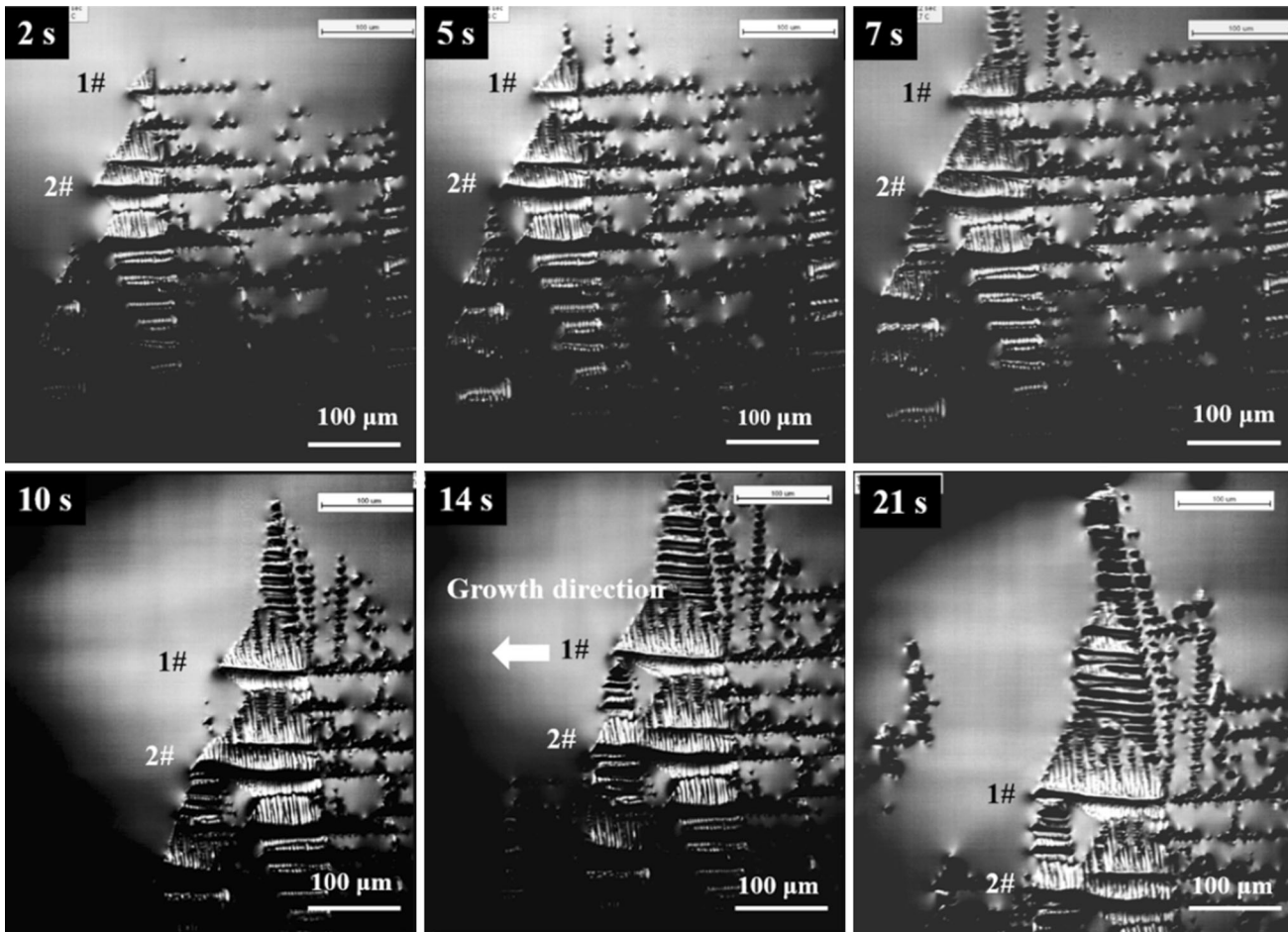


Fig. 5—The growth process of perovskite dendrites observed through CSLM.

surface, which showed the intact three dimensional perovskite dendrite structure as shown in Figure 8.

To conveniently describe the observed dendritic growth with time, the start time of the disquisitive dendritic growth was artificially set as the beginning of the video. The number 1 and 2 primary dendrites in Figure 5 were selected to evaluated the growth rate during isothermal holding through the images obtained from the *in situ* CSLM observation as follows.^[13] For example, for number 1 dendrite, the dendrite root is seen as the reference point (the right dash line). Then the position of the dendrite tip (the left dash line) was measured as the distance from the reference point (the distance of dash line with arrow) as time passes (Figure 9). The slope of the dendrite tip position as a function of time is then taken as the growth rate of the dendrite. Figure 10 shows the dendrite tip position in function of time of number 1 and 2 dendrites, and the slope determines the growth rates. It can be seen that the two dendrites show a linear growth at two stages, and they have a similar growth rate, indicating the similar temperature field and concentration field. In addition, the dendrites grow slower after 15 seconds at the second stage. After 40 seconds, dendrites almost stop growing. The growth rate of dendrites is controlled by the diffusion of solutes. The diffusion of solutes mainly

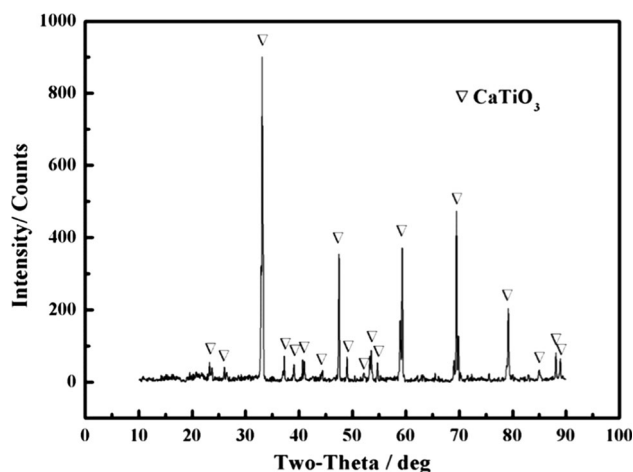


Fig. 6—The XRD pattern of slag sample isothermally crystallized at 1698 K (1425 °C).

depends on the gradients in liquid that are caused by the temperature difference and concentration difference in the interface area. At a constant temperature, the redistribution of solutes happens during solidification to reach the equilibrium of interface. When distribution coefficient k is less than 1, the solubility of solutes in solid is lower than in liquid, which leads to the enrichment of solutes at the interface. The enrichment of solutes decreases the concentration gradient in the liquid and thus decreases the diffusion rate of solute.^[18] In addition, the concentration of solutes in the liquid decreases with the solidification, which slows down the growth rate of solid.

B. Growth Mechanism of Perovskite Dendrites

The growth mechanism of perovskite was investigated by using the binary alloy crystallization model based on

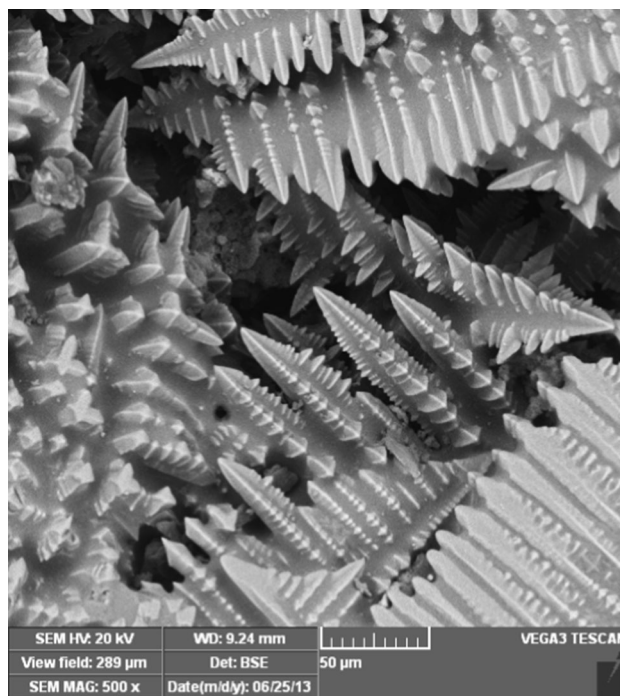


Fig. 8—The SEM image of the intact three-dimensional perovskite dendrites structure.

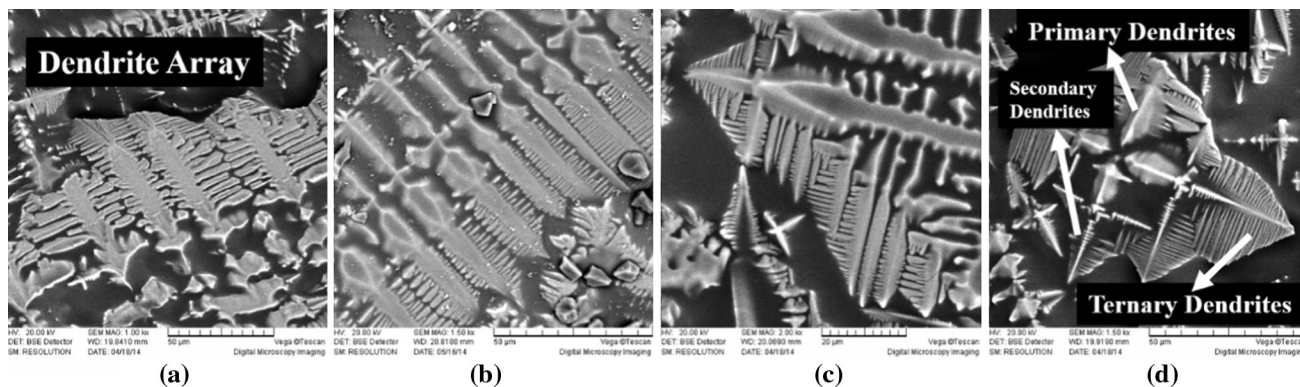


Fig. 7—The SEM images of perovskite dendrites.

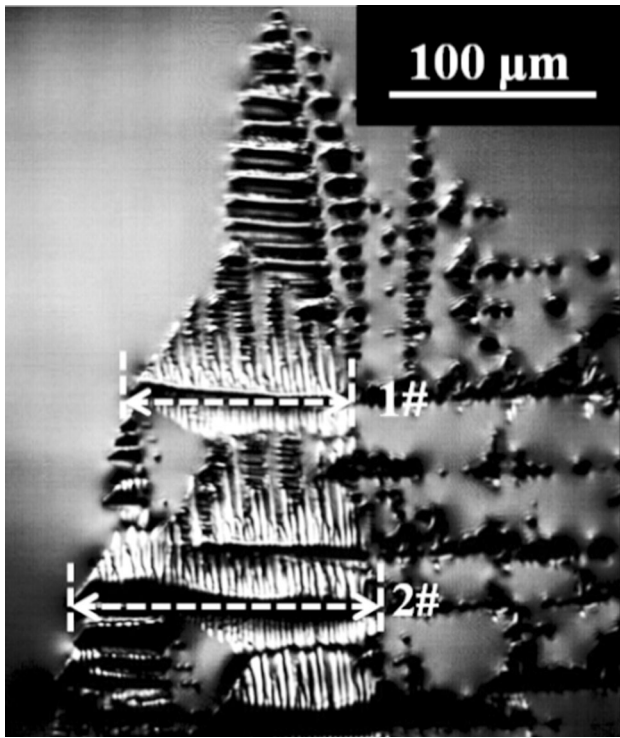


Fig. 9—Illustration of growth velocity measurement of perovskite dendrites.

the classic solidification theory. Primarily, the distribution of temperature field and concentration field of the growing dendrite tips should be discussed.

Based on the CSLM observation, the nucleation was not observed in non-isothermal crystallization or isothermal crystallization. In nonisothermal crystallization under continuous-cooling conditions mentioned before, the dendrites were presumed to nucleate and grow from the bottom of crucible, beneath the slag surface. In the current experiment, dendrites were seen growing to the viewing field from the edge possibly because the bottom and side of the crucible had a lower temperature or heterogeneous nucleation was easier on the crucible. However, the viewing field of CSLM, which was set up to the flat center of slag surface to ensure a clear vision, was limited and inconsistent with the nucleation spots.

The temperature difference between slag surface and crucible bottom was calculated based on heat transfer by Eq. [1].^[14] As mentioned before, heating in the infra furnace is achieved by radiation of heat from the golden cladding layer on the inner oval furnace chamber. The heat directly focuses on the slag surface and then conducts to the bottom and radiates away from the crucible bottom (Figure 11). At thermal equilibrium, the heat conducted to the crucible bottom and radiating away from the bottom should be balanced as shown in Eq. [1]. The slag is assumed to transmit no radiation. Argon in the furnace is assumed to conduct no heat because argon is a low-conductive gas and radiation is much more important than conduction at a high temperature. The temperature of slag surface is set as

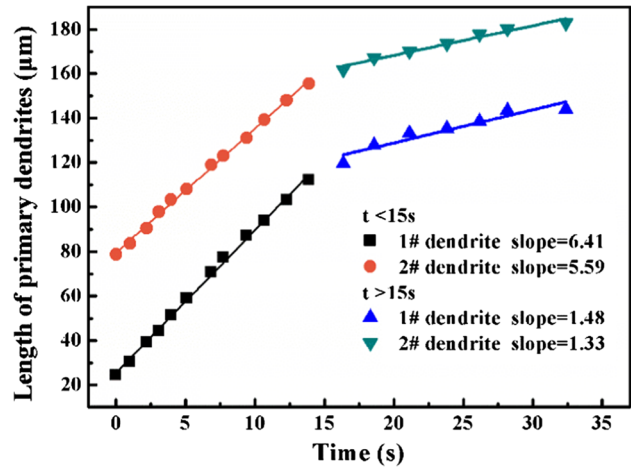


Fig. 10—Dendrite tip position as a function of time for perovskite at 1698 K (1425 °C).

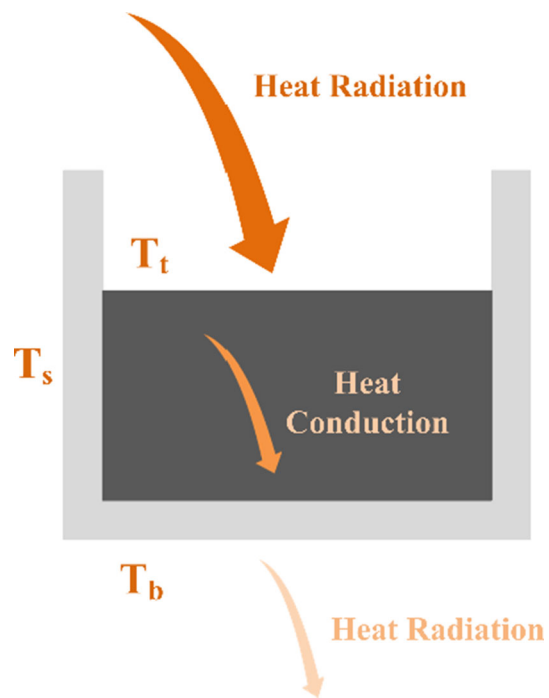


Fig. 11—Schematic diagram of heat transfer in slag sample.

1773 K (1500 °C) (T_t , this value is set as the highest temperature in the CSLM experiment), the temperature of bottom is calculated by the following equation:

$$k(T_t - T_b) \frac{A}{h} = \zeta \sigma AT_b^4. \quad [1]$$

The related calculation parameters and values are shown in Table III. Consequently, the bottom temperature was lower, about 71.3 K (71.3 °C), than the surface temperature of the slag, and the side temperature is lower. As a result, when the slag was cooled, because of the lower temperature of crucible, perovskite crystals first nucleated on the crucible side and bottom,

Table III. The Parameters and Value for Heat Balance Calculation of Slag Bottom

Parameter	Value	Physical Meaning
k	4 W/mK ^[15,16]	slag thermal conductivity
σ	5.669E-8 W/(m ² K ⁴) ^[15]	constant
ξ	0.2 ^[17]	emissivity of platinum
h	0.003 m	height of slag
A	5.024E-5 m ²	area of base
T_t	1773 K (1500 °C)	temperature of slag surface
T_b	1701.7 K (1428.7 °C)	temperature of slag bottom
ΔT	71.3 K (71.3 °C)	difference of T_t and T_b
T_s	1737.35 K (1464.35 °C)	temperature of slag side presume $T_s = (T_t + T_b)/2$

then grew toward the preferred crystallographic direction. The ideal crystallographic structure of perovskite is cubic, so crystals grow along $\langle 001 \rangle$ preferentially. The dendrites whose preferred crystallographic direction is opposite to the heat flow direction grow faster and finally present the columnar dendrite structure as show in Figures 5, 7, and 8.^[18]

Based on the theoretical isothermal phase composition diagram shown in Figure 2, it can be seen that four phases will form during cooling (Table I). The crystallization of perovskite (CaTiO_3) starts at 1709 K (1436 °C) and ends at about 1373 K (1100 °C). But the amount of perovskite remains steady almost below 1473 K (1200 °C) and its formation consumes most of CaO and TiO_2 . Because some CaO and TiO_2 are predicted to form clinopyroxene and TiO_2 , respectively, not all the CaO and TiO_2 will form the solid perovskite. Here, we only discuss the crystallization of perovskite between 1473 K and 1709 K (1200 °C and 1436 °C). Above 1473 K (1200 °C), titania spinel starts to form at 1598 K (1325 °C), but to simplify the case, its existence is ignored because the amount is so little. The existence of clinopyroxene is ignored as well for the same reason. Therefore, perovskite is assumed to be the only phase crystallizing between 1709 K and 1473 K (1436 °C and 1200 °C) with the approximate final amount of 34 pct in the slag.

The growth of perovskite dendrites follows the classic solidification theory proposed by Kurz and Fisher.^[18] To simplify the situation, the molecular theory of slag is employed to discuss the growth process of perovskite. Therefore, the initial liquid slag is considered to be made up of the oxides TiO_2 -CaO- SiO_2 - Al_2O_3 -MgO.^[19] As far as the formation of perovskite is concerned, it requires the diffusion of CaO and TiO_2 to the solid/liquid interface and the rejection of SiO_2 , Al_2O_3 , and MgO from the interface, as well as CaO and TiO_2 that are not involved in the solid formation. The total of SiO_2 , Al_2O_3 , MgO, CaO, and TiO_2 that are not involved in the solidification are called B in the following. Because the molar ratio of TiO_2 to CaO in solid perovskite is 1, TiO_2 and CaO in solution will diffuse simultaneously to the interface against the other oxides and solidify at the interface to form solid perovskite as shown in Figure 12.

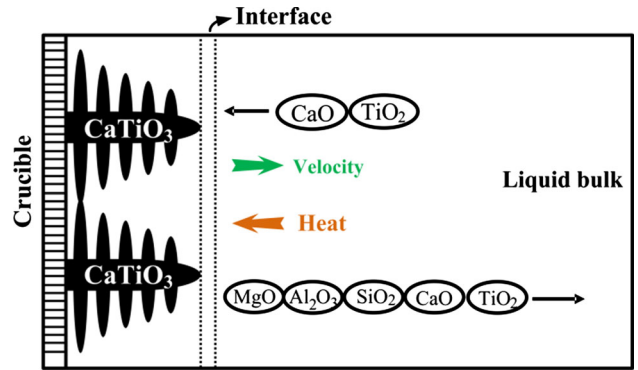


Fig. 12—Schematic diagram of growth process of perovskite dendrites.

However, as mentioned before, the redistribution of solutes leads to the enrichment of solutes at the interface, which will thus influence the liquidus temperature.

Because B does not form the solid phase of perovskite, it can be considered as an “inert phase” as far as solidification of perovskite is concerned between 1709 K and 1473 K (1436 °C and 1200 °C). Then, the initial liquid slag is considered to be made up of CaTiO_3 (CaO and TiO_2 with molar ratio of 1) and B. Hence, the slag is regarded as a binary component system “P-B” just like a binary alloy. The solidification of alloy is controlled by diffusion, and the columnar crystals grow as dendrites, which is corresponding with this case.

Based on the theoretical calculation in Figure 1 and Table II, the solid/liquid equilibrium schematic diagram (Figure 1(a)), a schematic representation of the constitutional undercooling and a schematic description of concentration field at interface in binary “P-B” system are made based on the calculation and described in Figure 13 (Figure 13 is a reconstruction of Figure 3.4 and Figure 4.8 in Reference 18). The abscissa in Figure 13(a) represents the wt pct of B in the liquid slag. With the solid perovskite forming, the B wt pct increases in the liquid slag and the liquidus temperature of the residual liquid slag decreases. Based on Table I, assume the total amount of solid perovskite that can form is 34 pct (0.25 mol), and the initial liquid slag, a “P-B” binary system, consists of 34 wt pct perovskite and 66 pct B above the crystallization temperature [1709 K (1436 °C)]. The crystallization of perovskite ends up at 1473 K (1200 °C), and at this temperature all the perovskite has been solidified from the liquid slag, leaving only B in the liquid slag. Therefore, the final liquid slag composition is 0 pct perovskite and 100 pct B. The liquidus is approximated to a straight line. The solid composition is always 100 pct perovskite (0 pct B), but not C_0 .

As a result, C_s is 0, and the composition of the slag at the interface will be determined from the phase diagram at the interface temperature, assuming equilibrium at the interface. The position of dendrite tip is set to be 0 on the horizontal axis, and z represents the distance away from the dendrite tip. C_1 is close to C_0 when z approaches infinity.

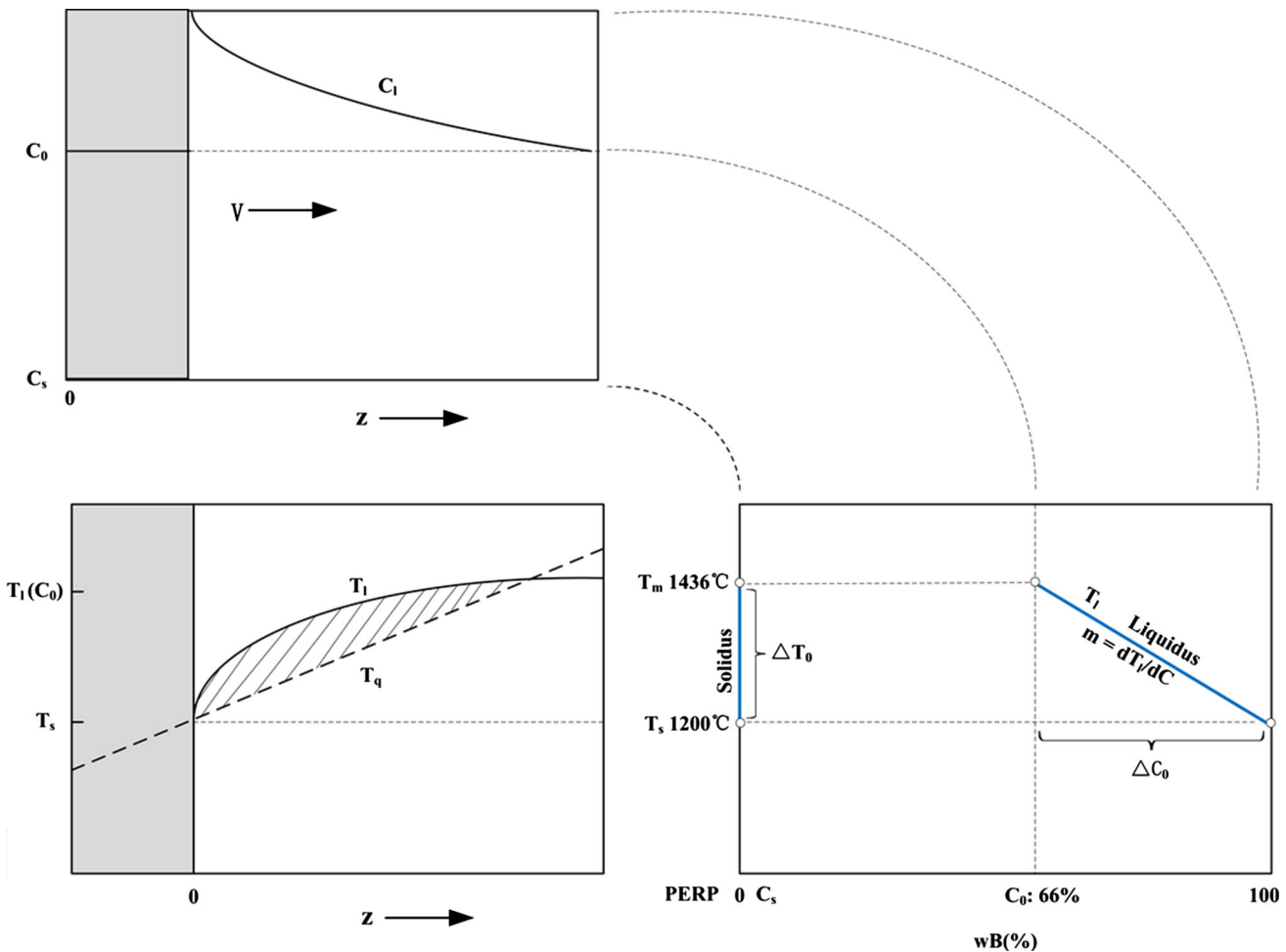


Fig. 13—The solid/liquid equilibrium schematic diagram, schematic representation of the constitutional undercooling, and schematic description of concentration field at interface in binary “P-B” system.

Assume that the solid and liquid have the same actual temperature gradient T_q . Solidification of perovskite makes the slag at the moving dendrite tip interface have lower amounts of TiO_2 and CaO , as well as a lower liquidus temperature (T_l) than the bulk slag. With a lower actual temperature gradient in the liquid, the interface is constitutionally supercooled, which drives the dendritic growth.

where T_m is the melting point of slag with C_0 , T_l is the liquidus temperature, T_s is the solidus temperature, T_q is the measurable temperature, m is the liquidus slope, C_0 is the initial concentration, C_s is the solid concentration, and C_l is the concentration at the solid/liquid interface.

IV. CONCLUSIONS

The isothermal crystallization of perovskite in TiO_2 - CaO - SiO_2 - Al_2O_3 - MgO synthesized high-titanium-bearing BF melt is observed *in situ* using a confocal scanning laser microscope at 1698 K (1425 °C). The growth mechanism of perovskite in melt is analyzed using solidification theory. The following conclusions are taken from this study.

The dendritic growth process of perovskite can be clearly observed through CSLM. The dendrite array grows

toward the same direction in which the primary dendrite trunks are parallel with each other. The secondary dendrite arms grow in the perpendicular direction with the primary trunk and stop growing when they encounter with each other. The perovskite dendrites show a linear growth at two stages. The dendrites grow faster at early stage at about 5 to 7 $\mu\text{m/s}$ and grow with a slower growth rate at about 1 to 2 $\mu\text{m/s}$ in later stage.

The growth of perovskite dendrites can be explained by the binary alloy crystallization model. The initial slag was considered as a binary component system in which one component is CaTiO_3 and the other component is the other species that does not form the solid perovskite. The formation of perovskite requires the diffusion of CaO and TiO_2 to the solid/liquid interface and the rejection of the other species from the interface. The solid/liquid equilibrium schematic diagram is made based on a theoretical calculation.

ACKNOWLEDGMENT

Project 51404044 was supported by National Natural Science Foundation of China. Project 20130191110015 was supported by Doctoral Fund.

ELECTRONIC SUPPLEMENTARY MATERIAL

The online version of this article (doi: [10.1007/s11663-015-0350-x](https://doi.org/10.1007/s11663-015-0350-x)) contains supplementary material, which is available to authorized users.

REFERENCES

1. X. Yao, L. Bin, and L. Chun: *Chin J. Process Eng.*, 2008, vol. 8 (6), pp. 1092–97.
2. Z.Z. Guo, T.P. Lou, L. Zhang, L.N. Zhang, and Z.T. Sui: *Acta Metall. Sin.*, 2007, vol. 20 (1), pp. 9–14.
3. L. Yuhai, L. Taiping, X. Yuhu, and S. Zhitong: *J. Mater. Sci.*, 2000, vol. 35 (22), pp. 5635–37.
4. L. Lu, H. Meilong, B. Chenguang, L. Xuewei, X. Yuzhou, and D. Qingyu: *Int. J. Min. Metall. Mater.*, 2014, vol. 21 (7), pp. 1–10.
5. S.S. Jung and I.L. Sohn: *Metall. Mater. Trans. B*, 2012, vol. 43B, pp. 1530–40.
6. S.S. Jung and I.L. Sohn: *J. Am. Ceram. Soc.*, 2012, vol. 96 (4), pp. 1309–16.
7. C. Orrling, S. Sridhar, and A.W. Cramb: *ISIJ Int.*, 2000, vol. 40 (9), pp. 877–85.
8. A. Semykina, J. Nakano, S. Sridhar, V. Shatokha, and S. Seetharaman: *Metall. Mater. Trans. B*, 2011, vol. 42B, pp. 471–6.
9. S. Sridhar and A.W. Cramb: *Metall. Mater. Trans. B*, 2000, vol. 31B, pp. 406–10.
10. H. Meilong, L. Lu, L. Xuewei, B. Chenguang, and Z. Shengfu: *Metall. Mater. Trans. B*, 2014, vol. 45B, pp. 76–85.
11. FactSage, www.factsage.com is a thermochemical software and database package developed jointly between Thermfact/CRCT (Montréal, Canada; www.crct.polymtl.ca) and GTT-Technologies (Aachen, Germany; www.gtt-technologies.de).
12. R. Trivedi and W. Kurz: *Int. Mater. Rev.*, 1994, vol. 39 (2), pp. 49–74.
13. L. Jingjing, C. Gong, Y. Pengcheng, P. Bart, M. Nele, and G. Muxing: *J. Cryst. Growth*, 2014, vol. 402, pp. 1–8.
14. Z. Guangjun: *Transfer Principle*, Metallurgical Industry Press, Beijing, 2009.
15. D.R. Poirier and G.H. Geiger: *Transport Phenomena in Materials Processing*, TMS, Warrendale, PA, 1994.
16. F. Jiangwen, H. Ying, C. Wei, Z. Liqing, and Z. Haohua: *J. Shenyang Normal Univ.*, 2010, vol. 28, no. 4, pp. 496–98.
17. H. Lvping: *Laser Infrared*, 1982, no. 4, pp. 65–7.
18. W. Kurz and D.J. Fisher, eds.: *Fundamentals of Solidification*, Higher Education Press, Beijing, 2010.
19. X. Huang: *Iron and Steel Metallurgy Principle*, Metallurgical Industry Press, Beijing, 2008, pp. 163–65.